Gas-phase electrocatalytic conversion of CO_2 to chemicals on sputtered Cu and Cu-C catalysts electrodes

N. Gutiérrez-Guerra[a], J. A. González[b], J.C. Serrano-Ruiz[c], E. López-Fernández[a] , J.L. Valverde[a], A. de Lucas-Consuegra[a,*]

[a] *Departamento de Ingeniería Química, Facultad de Ciencias y Tecnologías Químicas, Universidad de Castilla-La Mancha, 13071 Ciudad Real, Spain*

[b] *Instituto Regional de Investigación Científica Aplicada (IRICA) and Departamento de Física Aplicada, Universidad de Castilla-La Mancha, 13071 Ciudad Real, Spain*

[c] *Departamento de Ingeniería, Universidad Loyola Andalucía, Energía Solar, 1. Edifs. E, F and G, 41014, Seville, Spain*

[*]Corresponding author. Tel.: +34-926-295300; Fax: +34-926-295437;

E-mail address: Antonio.Lconsuegra@uclm.es (A. de Lucas-Consuegra).

ABSTRACT

A novel gas-phase electrocatalytic cell containing a low-temperature proton exchange membrane (PEM) was developed to electrochemically convert CO_2 into organic compounds. Two different Cu-based cathode catalysts (Cu and Cu-C) were prepared by physical vapor deposition method (sputtering) and subsequently employed for the gas-phase electroreduction of CO_2 at different temperatures (70–90 °C). The prepared electrodes Cu and Cu-C were characterized by X-ray diffraction (XRD), X-ray photoemission spectroscopy (XPS) and scanning electron microscopy (SEM). As revealed, Cu is partially oxidized on the surface of the samples and the Cu and Cu-C cathodic catalysts were comprised of a porous, continuous, and homogeneous film with nanocrystalline Cu with a grain size of 16 and 8 nm, respectively. The influence of the applied current and temperature on the electro-catalytic activity and selectivity of these materials was investigated. Among the two investigated electrodes, the pure Cu catalyst film showed the highest CO_2 specific electrocatalytic reduction rates and higher selectivity to methanol formation compared to the Cu-C electrode, which was attributed to the higher particle size of the former and lower CuO/Cu ratio. The obtained results show potential interest for the possible use of electrical renewable energy for the transformation of CO_2 into valuable products using low metal loading Cu based electrodes (0.5 mg Cu cm^{-2}) prepared by sputtering.

Keywords: CO_2 valorization; Electro-reduction; Cu catalyst; PEM; Selectivity; Methanol production

1. Introduction

Over the past centuries, the concentration of CO_2 in the atmosphere has rocketed, resulting in higher global temperatures and the associated climate change issues [1–3]. Thus, reducing CO_2 emissions is an extensive and long-term task, and three possible strategies have been proposed: (i) reduction of the amount of CO_2 released by increasing the energy efficiency or changing the primary energy source; (ii) capture and subsequent geological sequestration; and (iii) conversion of CO_2 into useful fuels and chemicals [1,4]. However, there are certain barriers (e.g., high cost of CO_2 capture, separation, purification, and transportation) that hinder the practical valorization of CO_2. Furthermore, the high energy requirements for CO_2 chemical/electrochemical conversion and the limitations of the market size and investment incentives are technological challenges to be overcome [1]. Despite these issues, global energy demands suggest that the conversion and the utilization of CO_2 is the most attractive and promising solution. Usually, CO_2 conversion can be achieved via chemical [5–7], photocatalytic [8,9], electrochemical [10,11], biological [12], reforming [13], and inorganic methods [14]. Among them, the electrochemical reduction of CO_2 has been recognized as an efficient route for converting CO_2 into energy-rich products. This process has a number of advantages: (i) it can be controlled by the electrode potentials and the reaction temperature; (ii) the supporting electrolytes can be fully recycled, thereby limiting the consumption of chemicals to simply water or wastewater; (iii) the electrochemical reaction systems are typically compact, modular, on-demand, and easily scalable; and (iv) the electricity used to drive the process can be obtained from a renewable sources. In this way, renewable energy can enter in the value chain of chemical industries. Nearly most of the studies on electrochemical reduction of CO_2 are carried out in the presence of a liquid (aqueous or organic) electrolyte [15–17]. However, the recovery of the reaction products from the liquid electrolyte is the main drawback of these processes, since the energy required to separate the products is higher than the energy stored in the produced molecules [8]. In this sense, gas-phase processes have advantages over the liquid-phase ones because in the former the solubility of CO_2 is not limited by the liquid medium and it is possible to obtain longer hydrocarbon chains [8]. Gas-phase processes involve a low-temperature proton exchange membrane (PEM) reactor configuration consisting of a membrane-electrode assembly (MEA, anode/membrane/cathode). As previously reported [8,18–24], several products (e.g., CO, methane, methanol, ethanol, formate, n-propanol, isopropanol, allyl alcohol, acetaldehyde, acetate, and ethylene glycol, among others) can be obtained via gas-phase electrochemical reduction of CO_2 following the overall scheme:

$$xCO_2 + 2(2x - z + y/2)H^+ + 2(2x - z + y/2)e^- \rightarrow C_xH_yO_z + (2x - z)H_2O \quad (1)$$

Among these products, methanol is particularly interesting as an energy vector. Methanol is a primary petrochemical product, which is of considerable importance in the chemical and energy industries due to its easy storage and transportation. Methanol is commonly used as a solvent and feedstock for the production of a number of chemicals (e.g., formaldehyde, acetic acid, methyl methacrylate, dimethyl terephthalate, methylammines, and chloromethanes) and fuel additives (e.g., methyl tertiary butyl ether and fatty acid methyl esters) [25]. Ethylene and propylene can be produced from methanol through the methanol-to-olefins process and used subsequently for producing polymers and hydrocarbons fuels [26]. Methanol can be also used in fuel cells [27] and represents an excellent alternative to combustion engine fuels [28]. Owing to their high activity and selectivity towards methanol, Cu-based catalysts have been extensively studied in catalytic hydrogenation [29–31] and electrocatalytic processes [18]. In most of the previous studies, impregnation procedures have been reported for the preparation of the catalysts.

In this work, we propose the use of physical vapor deposition methods, such as the sputtering technique directly applied onto the carbon cloth gas diffusion layer (GDL), for the preparation of catalysts to be used in the gas-phase electrocatalytic conversion of CO_2 to chemicals. This deposition technique, which has been previously used for preparing electrodes in other applications [32], has several advantages since it allows: (i) deposition of pure metallic films with high dispersion; (ii) deposition of very thin films with precise control of the thickness; (iii) good adhesion of the metal film to the substrate; (iv) easy and reproducible scale-up. In this sense, we report herein a novel electrochemical cell based on a low-temperature proton exchange membrane (PEM) reactor configuration. We conducted gas-phase electroreduction of CO_2 into high added-value products without feeding hydrogen on Cu and Cu–C cathodic catalysts prepared by the sputtering technique. The deposited electrodes were characterized and tested in the electrocatalytic conversion of CO_2 under a number of different reaction conditions. The obtained promising results showed the interest of using this kind of preparation procedures for electrocatalytic applications.

2. Experimental

2.1. Electrochemical catalyst preparation

Copper (Cu) and copper-carbon (Cu-C) materials supported on carbon paper served as the cathode of the electrocatalytic reactor, while IrO_2 supported on carbon was used as the anode.

The Cu and Cu-C cathodic catalysts were deposited by magnetron sputtering on carbon paper (Fuel Cell Earth) substrates at a rate of 0.81 nm/s with thicknesses of 500 and 1014 nm, respectively, as revealed by environmental scanning electron microscopy (ESEM, data not shown). Thus, metal loadings of around 0.5 mg/cm^2 Cu were obtained in both samples for the Cu based cathodic catalysts. The deposition was performed at a constant power of 50 W (Cu) or 100 W (Cu-C) in a vacuum chamber at base and working pressures of 3×10^{-7} and 3×10^{-3} mbar of 99.999% pure Ar, respectively. In the case of the Cu-C alloy, the proper composition was achieved by the co-sputtering of Cu and C from a pure graphite target having small pieces of copper stuck to it. The composition of the Cu-C cathodic-catalyst was determined on a scanning electron microscope equipped with an energy-dispersive X-ray (EDX) detector. Different measurements taken within a large area yielded an average composition of 70% Cu and 30% C, both within a 1% error.

The anode catalyst ink was prepared by mixing appropriate amounts of IrO_2 commercial catalyst powders (Alfa Aesar, 99%) with a Nafion solution (Aldrich chemistry, Nafion® 117 solution) and isopropanol (Sigma Aldrich). IrO_2 has been widely used in PEM water electrolyzers owing to its unique and superior performance towards the water oxidation reaction as compared to non-noble metal catalysts (e.g., Ni, Co and Cu) and noble metal electrocatalysts such as Pt [33]. The ink was subsequently applied on a carbon paper substrate at 65 °C to reach a metal loading of 0.5 mg/cm^2 for the anode after drying. The geometric surface area of both electrodes was 12.56 cm^2 (circular electrode of 4 cm in diameter).

A proton-conducting Sterion® membrane of 185 μm in thickness (supplied by Hydrogen works) was used as the electrolyte (i.e., H^+ conductor material). Prior to use, the Sterion® membrane was successively immersed at 100 °C for 2 h in H_2O_2 (to remove organic impurities), H_2SO_4 (for activating the membrane) and deionized water (to remove traces of solutions). Finally, a membrane electrode assembly (MEA) was prepared upon hot-pressing (1 ton) at 120 °C for 3 min the two electrodes sandwiching with the membrane.

2.2. Catalytic activity measurements

The CO_2 electroreduction experiments were carried out in a lab-scale (electrode of 4 cm in diameter) continuous electrocatalytic reactor operating at atmospheric pressure. The cell reactor was made of two quartz tube (cathodic and anodic compartments) with two inlets (CO_2 and H_2O/N_2) and two outlets. It has been described in detail elsewhere [34].

Water was introduced into the anodic chamber by flowing N_2 through a saturator operating under liquid/vapor equilibrium conditions. The water content in the anodic chamber (25% H_2O/N_2) was controlled by the water vapor pressure which is in turn controlled by the temperature of the saturator (65 °C). All lines downstream the saturator were heated above 100 °C to prevent condensation. Water oxidation was carried out over the IrO_2 anode leading to the formation of H^+ and O_2. Protons are subsequently transported across the Sterion® membrane. Furthermore, water was fed to hydrate the Sterion® membrane and keep its proton conductivity properties [18]. The output of the anodic side (O_2) was released to the atmosphere. The cathodic part of the cell operated in contact with a gas flow of pure CO_2 (Praxair, Inc. certified standards 99.999% purity). Both gas flow rates (N_2 and CO_2 for the anode and cathode,

118 respectively) were controlled by a set of mass flowmeters (Brooks 5850 E and 5850 S). The electrocatalytic
119 experiments were carried out at atmospheric pressure with an overall gas flow rate of 0.5 NmL/min of CO_2 for the
120 cathode and 6 NmL/min for the anodic stream (25 % H_2O/N_2). The reaction was carried out at different temperatures
121 (70 and 90 °C, optimum values for the operation of the Sterion membrane). The reactant and products released in the
122 cathodic chamber were analyzed in a double channel gas chromatograph (Bruker 450-GC) equipped with Hayesep Q-
123 Molsieve 13X consecutive columns and flame ionization detectors. The main reaction products detected were: H_2,
124 CH_4, methanol, and acetaldehyde (see supporting information, Fig. S1). A potentiostat/galvanostat (Voltalab 21,
125 Radiometer Analyticall) was used to supply a constant current (−10 to −30 mA) between the electrodes, which were
126 connected using gold wires.

127 *2.3. Characterization of the Cu catalyst-electrodes*

128 The Cu electrodes were characterized by X-ray diffraction (XRD) on a Philips PW-1710 instrument using Ni-
129 filtered Cu *K*α radiation (λ = 1.5404 Å). The samples were scanned at 0.02°/step over the range $20° \leq 2\theta \leq 90°$ (scan
130 time 2 s/step) and the diffractograms were compared with JCPDS-ICDD references. X-ray photoelectron
131 spectroscopy (XPS) was performed with a PHOIBOS-100 spectrometer with delay line detector (DLD) from SPECS,
132 which worked in the constant pass energy mode fixed at 30 eV. The morphology of the Cu electrodes was also
133 characterized by ESEM using a Quanta 250 device (FEI Company). This instrument was connected to an EDAX
134 Apollo X (AMETEK) analyser, which analyzes the chemical composition of the electrodes by dispersive X-ray
135 analysis (EDAX). Cyclic voltammetry experiments were also conducted with the potentiostat/galvanostat (Voltalab
136 21, Radiometer Analyticall) at a scan rate of 80 μA/s under different gas phase conditions.

137 **3. Results and discussion**

138 *3.1. Characterization of the Cu cathodic catalysts*

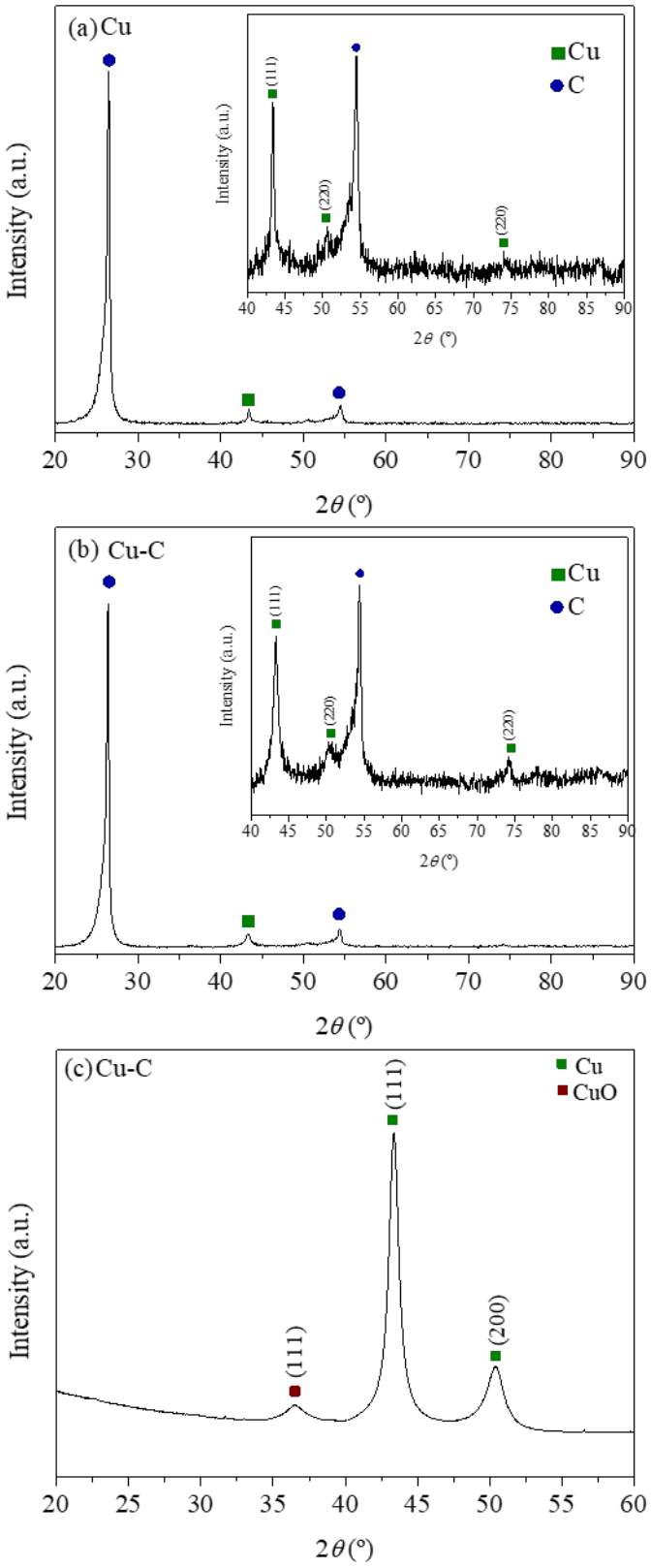

Fig. 1. XRD analysis patterns of Cu cathodic-catalyst on carbon paper substrates (a), Cu-C cathodic-catalyst on carbon paper substrates (b), and Cu-C on Si substrate (c), prepared by sputtering. Insets of (a) and (b) show the magnification of XRD patterns of Cu cathodic-catalyst and Cu-C cathodic-catalyst, respectively.

As shown in Fig. 1(a, b), two peaks at ca. $2\theta = 25°$ and 55° were observed, which could be associated with the carbon paper used as a current collector. This fact was corroborated by the XRD pattern of this material (not shown here). The main diffraction peaks at $2\theta = 43.3°$, 50.4° and 74.1° were associated to the (111), (200), and (220) crystallographic planes of metallic copper with a face-centred cubic (FCC) crystalline structure (JCPDS, 85-1326) (Insets of Fig. 1a,b). As it can be seen, no peaks corresponding to the carbon phase were observed for the Cu-C cathodic-catalyst (Fig. 1b), in line with the results reported by Pauleau et al. [35] for copper-carbon composite films deposited on silicon substrates by sputtering. This fact was corroborated by the XRD pattern of the Cu-C cathodic catalyst separately deposited over a Si substrate (Fig. 1c). The XRD pattern of the Cu-C cathodic catalyst films exhibited only diffraction peaks produced by copper phases, including a peak ascribed to the (111) plane of CuO (JCPDS, 80-1917) which indicate that Cu may be partially oxidized, probably at the surface. No peaks associated to carbon were detected, which can be attributed to the small particle size of C compared to that of Cu. Thus, carbon particles might be inserted into the copper lattice in a disordered manner, avoiding their detection by XRD. The slight shift towards lower 2θ values of the peaks of Cu-C versus those of the Cu cathodic catalyst support this hypothesis. Thus, this shift reveals a lattice expansion arising from the incorporation of small C atoms into the Cu lattice [36]. The main Cu diffraction peak at $2\theta = 43.3°$ was used to determine the Cu crystal size via the Scherrer's equation. The values obtained: 16 and 8 nm for the Cu and Cu-C catalysts, respectively, are of the same order than those previously reported for sputtering-derived Cu electrodes [35,37,38]. In line with the results reported by Pauleau et al. [35], the incorporation of carbon in the structure of Cu resulted in lower Cu particle sizes, since carbon hinders the growth of the copper crystal grains during the catalyst film preparation procedure. XPS measurements were also performed on both cathodic catalysts. Fig. 2 shows the Cu_{2p} transition for the Cu (Fig. 2a) and Cu-C (Fig. 2b) electrodes. In good agreement with the XRD analysis, the Cu_{2p} signal revealed a mixture of Cu and CuO species on the cathode surface for both catalysts. This partial surface oxidation of Cu may have taken place by direct contact of the electrodes with air during the transport of the sample to the electrochemical cell reactor. The CuO/Cu ratio seems to be higher for the Cu-C electrode vs. the pure Cu electrode. This can be attributed to the lower Cu crystallite size of the former material, which might have facilitated Cu surface oxidation in contact with air.

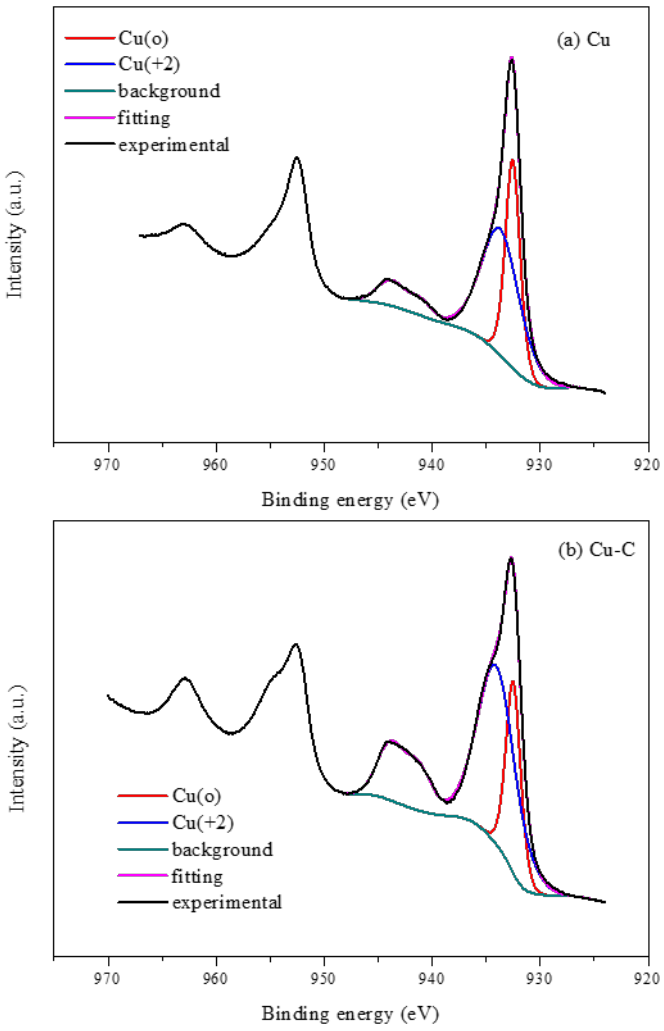

Fig. 2. XPS measurements of the Cu (a) and Cu-C (b) cathodic catalyst

The morphologies of the carbon paper substrates (Fig. 3a), Cu (Fig. 3b), and Cu-C (Fig. 3c) cathodic catalysts before the electrocatalytic tests were observed by ESEM. As shown in Fig. 3(b1, c1), the sputter-deposition process achieved a complete coverage of the carbon microfiber area exposed to the sputtered flux. This fact was confirmed by the ESEM micrographs of the carbon paper substrate (Fig. 3a). Thus, the sputtering method allowed to obtain thin metal films while maintaining the microstructure of the carbon paper support. Furthermore, as shown in Fig. 3(b1, c1), the films were homogeneous and did not lack continuity, as verified by the electrical conductivity measurements and the homogeneity of the formed Cu catalyst interconnected over the entire covered carbon paper surface area. The Cu catalyst expanded laterally from the carbon fibers, forming a self-standing macroporous membrane having most of its surface accessible to the reactive medium. Additionally, as clearly seen in the magnified images (Fig. 3b2, 3c2), the samples were porous, which facilitated the diffusion of reactants and products, while Cu grains were spherical. As anticipated by the XRD results, the Cu-C cathodic catalyst showed lower Cu grain sizes than Cu.

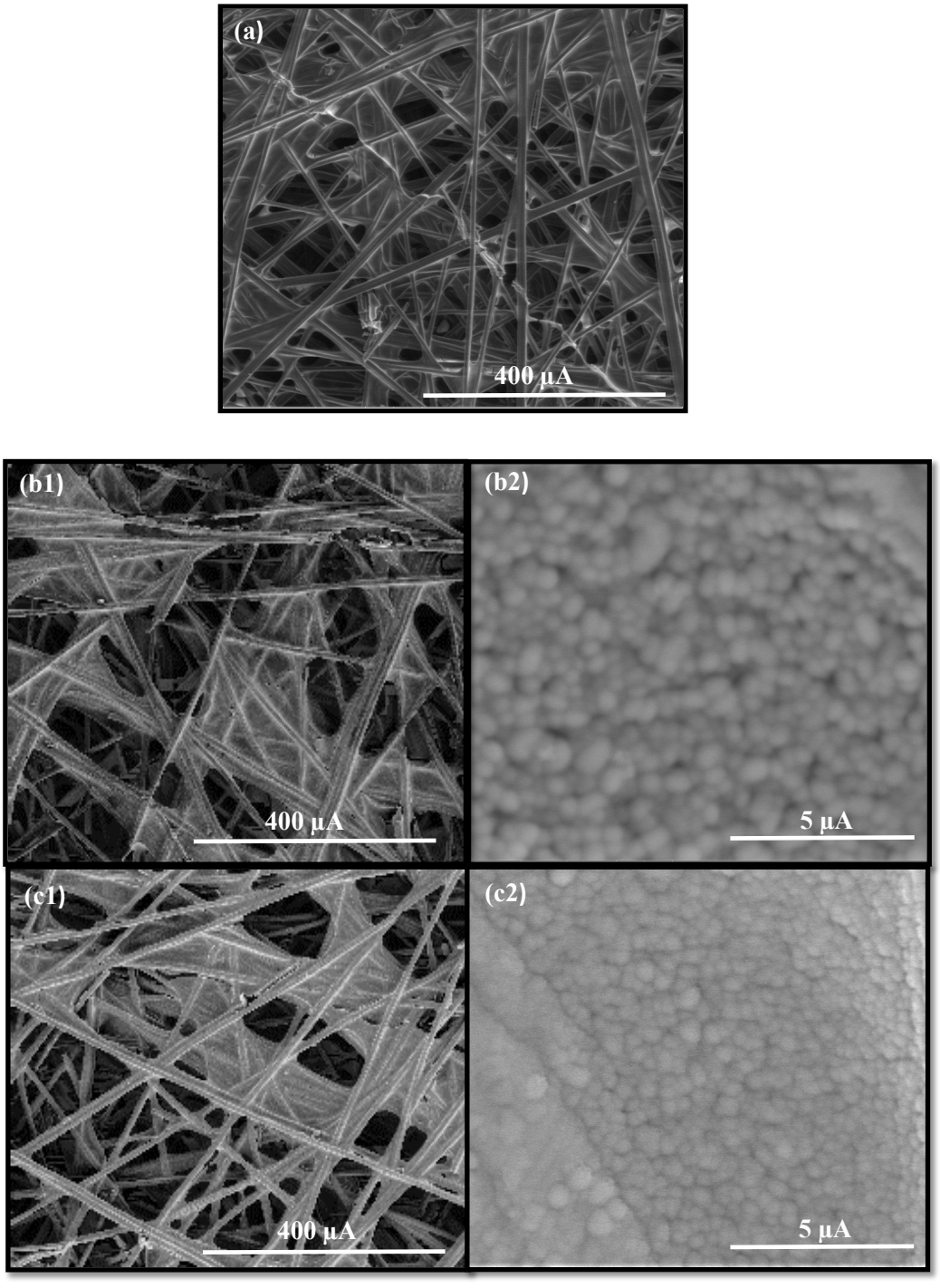

Fig. 3. SEM micrographs of the carbon paper substrates (a), and cathodic catalyst Cu (b), and Cu-C (c) prepared onto them.

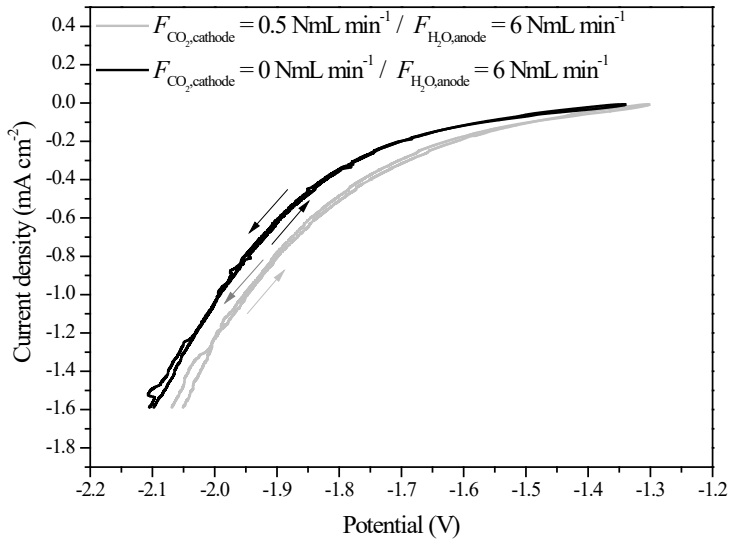

Fig. 4. Influence of the reaction atmosphere on the current density-potential curves obtained during a cyclic voltammetry. Conditions: Temperature = 90 °C, scan rate = 80 μA/s.

Prior to the catalytic activity measurements, the Cu/Sterion/IrO_2 and Cu-C/Sterion/IrO_2 MEAs were in situ characterized by cyclic voltammetry under the same electrochemical reaction conditions (i.e., $F_{CO_2,\ cathode}$ = 0.5 NmL/min, $F_{H_2O,\ anode}$ = 6 NmL/min) and without feeding CO_2 to the cell ($F_{CO_2,\ cathode}$ = 0 NmL/min, $F_{H_2O,\ anode}$ = 6 NmL/min) at 90 °C. The potential variation was recorded versus the applied current density (current range between 0 and −20 mA) with a scan rate of 80 μA/s (Fig. 4). The variation of the obtained current density with the applied potential for water ($F_{CO_2,\ cathode}$ = 0 Nml/min / $F_{H_2O,anode}$ = 6 Nml/min) was firstly obtained. As can be observed, water electrolysis started at −1.5 V (change of slope in the curve) in the anode side [39], according to the following reaction:

$$H_2O \rightarrow H^+ + ½\ O_2 + e^- \quad (2)$$

An increase in the applied current resulted in higher potential values (up to −2.1 V) and, hence, in an increase of the protons production rate.

In the cathodic side, hydrogen was obtained by the reaction of protons previously transported through the protonic membrane and electrons:

$$2H^+ + 2e^- \rightarrow H_2 \quad (3)$$

On the other hand, the current slightly decreased upon CO_2 feeding to the cathodic chamber ($F_{CO_2,\ cathode}$ = 0.5 Nml/min / $F_{H_2O,anode}$ = 6 Nml/min). The gas-phase reduction of CO_2 to liquid fuels and hydrocarbons is a complex multistep reaction involving shared intermediates and multiple reaction pathways [8,18−21]. The formation of different products in the cathodic side (i.e., methanol, acetaldehyde, and methane) can be explained according to the following reactions:

$$CO_2 + 6H^+ + 6e^- \rightarrow CH_3OH \quad (4)$$

$$CO_2 + 10H^+ + 10e^- \rightarrow CH_3CHO + 3H_2O \quad (5)$$

$$CO_2 + 8H^+ + 8e^- \rightarrow CH_4 + 2H_2O \quad (6)$$

CO_2 feeding resulted in lower cell potentials values (for the same current), demonstrating the electrochemical nature of the products formation reactions (Eqs. 4–6). Hence, the adsorption CO_2 on the Cu active sites from the gas phase facilitated the removal of H^+, acting as a depolarizing agent [40]. The use of different molecules as depolarizing agents has been previously applied to the electrolytic production of H_2 at high temperatures. In this regard, the use of CH_4 [41,42], CO [43], and C [40,41] has been reported to significantly decrease the required electrical power in electrolysis experiments. In short, the observed difference in the current-potential curves obtained under absence and presence of CO_2 can be attributed to the electrocatalytic activity of the Cu cathodic catalyst in the CO_2 electro-reduction (Eqs. 4–6) competing with the H_2 evolution reaction (Eq. 3).

3.2. Electrocatalytic reduction of CO_2 experiments

The formation rate of the products as a function of the reaction time for a constant applied current of −20 mA (j = −1.6 mA/cm^2) at 90 °C on the Cu/Sterion/IrO_2 electrochemical cell is depicted in Fig. 5. Under open circuit conditions (OCC, no current application), no products were obtained. Then, a constant current of −20 mA was applied for 235 min under the same reaction atmosphere. This polarization current value was maintained until a steady state value was reached. During this current imposition step, hydrogen (not shown here), methanol (Fig. 5a), acetaldehyde, and methane (Fig. 5b) were obtained via CO_2 electro-reduction on the Cu electrode. Most of these products had been already identified in similar studies involving electrocatalytic conversion of CO_2 [8,18–21]. During the first 200 minutes of reaction, the production rates of methanol, methane, and acetaldehyde were very similar. After 200 min, the methanol production rate progressively increased with the reaction time, becoming the main reaction product. The overall production rate reached a maximum after ca. 225 min of reaction decreased thereafter under open circuit conditions. The steady state regime was reached after 4–5 h of reaction. Finally, under OCC, the cathodic side of the cell was purged with N_2 (30 NmL/min) in order to remove all the products from the reactor. The variation of the potential as a function of time during the galvanostatic operation of the cell (−20 mA) is also depicted in Fig. 5(c). As can be seen, the potential rapidly decreased reaching a stable value of −2.1 V. This potential was stable during the negative polarization step showing the stability of the electrode.

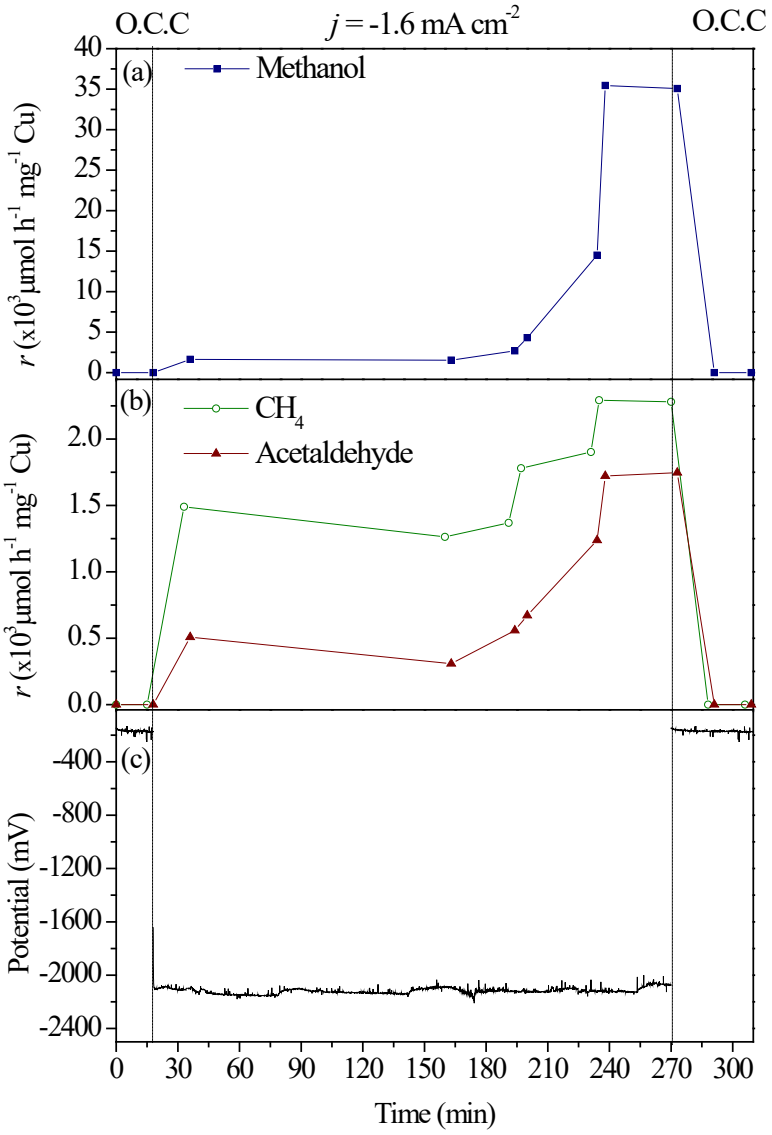

Fig. 5. Evolution of the rate of products as a function of time of reaction for an applied current density of j = –1.6 mA/cm^2 on Cu/Sterion/IrO_2 electrode. Conditions: Temperature = 90 °C, $F_{CO_2,cathode}$ = 0.5 NmL/min, $F_{CO_2,anode}$ = 6 NmL/min.

Fig. 6 compares the performance of the Cu/Sterion/IrO_2 (Fig. 6a) and Cu-C/Sterion/IrO_2 electrochemical cells (Fig. 6b) in the gas-phase reduction of CO_2 normalized per mg of Cu. The experiments were performed at 90 °C. Different current densities were applied (j = −0.8, −1.6, and −2.4 mA/cm^2). The increase in the applied current resulted in higher CO_2 consumptions rates due to the increase in the kinetics of the electrocatalytic reaction. In all the cases, the Cu-C cathodic catalyst showed lower specific reaction rates than the pure Cu electrode. The significantly higher activity for methanol formation observed for the catalyst having higher Cu crystal sizes could arise for the different structure of the large particles versus the small ones. Thus, large particles present different types of exposed planes or defects that could result in higher activities [44]. In addition, the higher CuO/Cu ratio of Cu-C vs. the pure Cu cathode may be responsible for the lower intrinsic electrocatalytic activity. On the other hand, as mentioned above, the main product of reaction, besides hydrogen, was methanol for the Cu/Sterion/IrO_2 electrode whereas minor amounts of other compounds such as acetaldehyde and methane were observed. The methanol production rates normalized per area of electrode (0.0224 and 0.0017 μmol/(cm^2 h) for Cu and Cu-C, respectively) at −10 mA (−0.8 mA/cm^2) were higher than those previously reported for the CO_2 electroreduction in the gas phase over Cu-carbon nanofiber catalysts prepared under similar conditions by typical impregnation methods (0.0088–0.0141 μmol/(cm^2 h)) [18]. This result shows the potential of the physical vapour deposition methods (such as the sputtering technique) for electrode preparation, which allows to prepare catalyst films of low metal loading, low particle size and high specific activity for electrocatalytic applications. On the other hand, it should be mentioned that although the type of products was similar for both catalysts (Cu and Cu-C), different products distributions were observed. When carbon was incorporated to the electrode (Cu-C), acetaldehyde was the main product for all the applied currents. This finding is also in agreement with previous studies of catalytic CO_2 hydrogenation, which have reported that higher Cu particle sizes are particularly selective towards methanol vs. acetaldehyde formation [44,45]. Previous works revised in detail elsewhere [18–22] have described in detail different mechanisms for the CO_2 electro-reduction reaction. For instance, it is interesting to note that the extent of products formation depends on the surface orientation of the copper electrode and different reaction pathways can be followed, leading to different reaction products. Since methanol, acetaldehyde, and methane were the main detected products herein, we believe that they are likely formed through the intermediate formation of CO^*_{ads} species instead of CO_2H_{ads} [23].

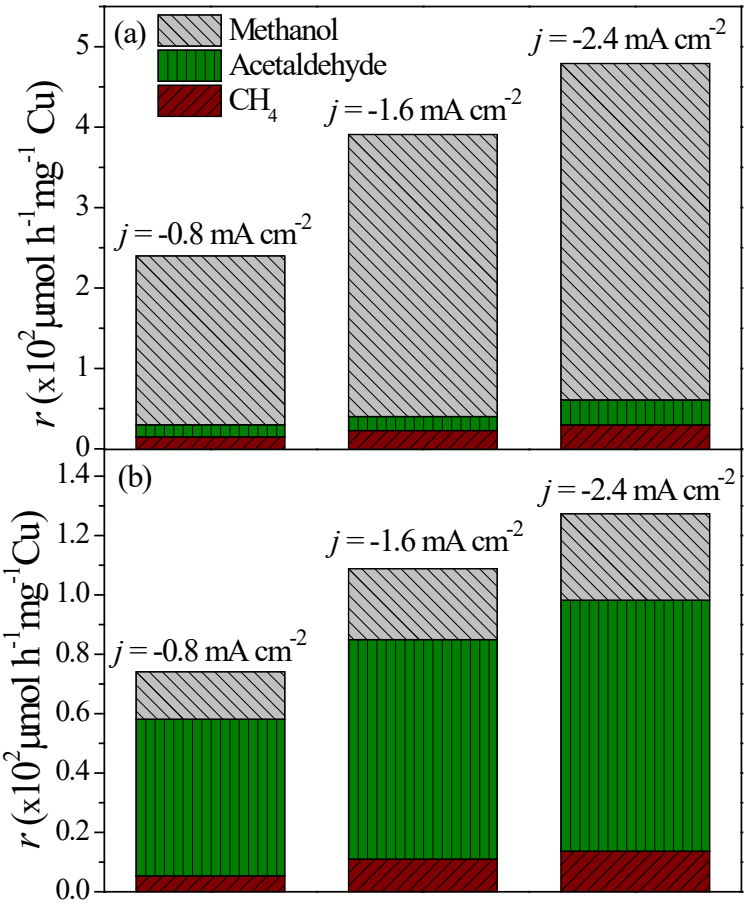

Fig. 6. Effect of the current density on the production rate in the electrocatalytic conversion of CO_2 on Cu/Sterion/IrO_2 (a) and Cu-C/Sterion/IrO_2 (b) electrodes. Conditions: Temperature = 90 °C, $F_{CO_2,cathode}$ = 0.5 NmL/min, $F_{CO_2,anode}$ = 6 NmL/min.

The effect of temperature on the CO_2 consumption rate at $I = -20$ mA ($j = -1.6$ mA/cm^2) for the Cu/Sterion/IrO_2 and Cu-C/Sterion/IrO_2 electrodes is depicted in Fig. 7. The CO_2 consumption rate was enhanced with increasing temperatures [8]. This phenomenon could be attributed to the increase of the kinetics of the electrochemical processes [46,47]. As mentioned before, the Cu/Sterion/IrO_2 electrode showed higher CO_2 consumption rates, although the effect of temperature seems to be less intense.

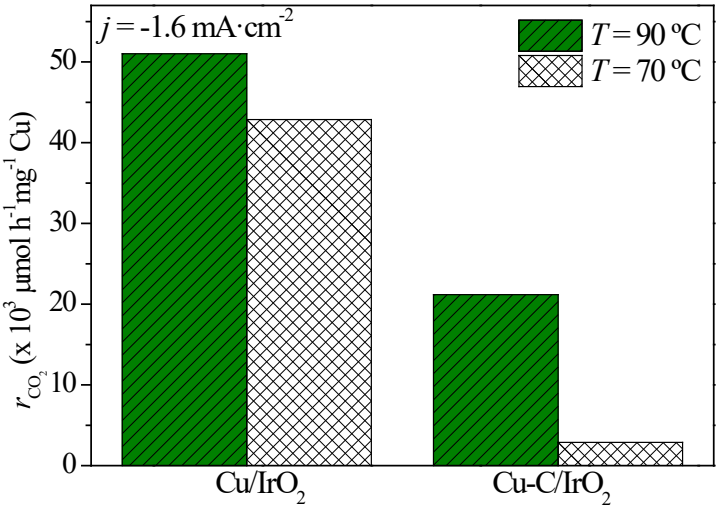

Fig. 7. Effect of temperature (T = 70 and 90 °C) on CO_2 consumption rate for Cu/Sterion/IrO_2 and Cu-C/Sterion/IrO_2 electrodes. Conditions: j = −1.6 mA/cm^2, $F_{CO_2,cathode}$ = 0.5 NmL/min, $F_{CO_2,anode}$ = 6 NmL/min.

Table 1 reports the selectivity towards methanol, acetaldehyde, and methane, excluding hydrogen, during the electrocatalytic conversion of CO_2 on Cu/Sterion/IrO_2 and Cu-C/Sterion/IrO_2 electrodes for the different experiments of Fig. 7. The selectivity of each compound was calculated as follows:

$$\text{Selectivity } x_i\ (\%) = \frac{F_{X_i}}{F^0_{CO_2} - F_{CO_2}} \times 100 \qquad (7)$$

As can be observed from Table 1, for the case of the Cu cathode an increase in the reaction temperature led to an increase in the selectivity towards methanol formation from 82% to 92% while an increase in the selectivity to methane (from 6% to 26%) was achieved for the case of Cu-C cathodic catalyst. Although higher number of experiments in a wider temperature range should been performed, in good agreement with previous studies [23] it could be generally observed that an increase in the reaction temperatures, favors the reaction pathways implying lower number of protons. Hence, there is relative increase of the kinetics of Eq. (4) (6 e^-) for the case of Cu and Eq. (6) (8 e^-) for the case of Cu-C cathodic catalyst, decreasing in both cases the selectivity towards CH_3CHO which implies a higher number of electrons (10 e^-, Eq. 5). At this point it should also be noted that low values of Faradaic Efficiencies to hydrocarbon products (below 10%) were obtained in all the experiments. This is due to the high kinetics of hydrogen evolution reaction (reaction 2) vs. hydrocarbon formation reactions (Eqs. 3–5) due to the low surface concentration of CO_2. However, under gas phase operations, the electrocatalytic reduction of CO_2 offer the potential advantage of an energy-saving recovery of the products of reaction, particularly when the aim is to form liquid fuels such as alcohols. This separation of liquid organics (e.g., methanol, acetaldehyde in our system) from hydrogen can be easily performed by the condensation of the products and hence, the selectivity towards the different obtained hydrocarbons, is the most important parameter. Then H_2 is still the main product of reaction and selective electrocatalysts will be required to inhibit the surface reaction toward H_2 formation, for example, by selective blocking the surface sites with strongly chemisorbed species or by modification of the electrocatalyst [18].

Table 1. Selectivity of methanol, acetaldehyde and methane in the electrocatalytic conversion of CO_2 on Cu/Sterion/IrO_2 and Cu-C/Sterion/IrO_2 electrocatalysts at different temperatures (T = 70 °C, T = 90 °C). Conditions: j = −1.6 mA/cm^2, $F_{CO_2,cathode}$ = 0.5 NmL/min, $F_{CO_2,anode}$ = 6 NmL/min.

Electrode	T (°C)	S_{CH_3OH} (%)	S_{CH_3CHO} (%)	S_{CH_4} (%)
Cu/Sterion/IrO_2	70	81.95	12.21	5.84
	90	92.76	1.91	5.33
Cu-C/Sterion/IrO_2	70	13.75	79.80	6.43
	90	14.05	60.17	25.78

4. Conclusions

The obtained results showed that the electrocatalytic reactor configuration used in this work may be of great interest for the electro-reduction of CO_2 in gas phase into high added-value compounds. The use of the physical vapour deposition methods for the electrode preparation such as the sputtering technique allowed to prepare catalyst films of low metal loading, low particle size and high specific activity for electrocatalytic applications (e.g. CO_2 electro-reduction). The use of Cu based sputtered electrodes allowed to achieve higher CO_2 specific electro-reduction rates with higher selectivities to methanol formation than those reported in previous studies. Among the two investigated electrodes Cu and Cu-C, the former one led to the highest electrocatalytic activity and selectivity towards methanol formation, which was attributed to its higher particle size and lower ratio of CuO/Cu. Both the applied current and the reaction temperature positively contributed to an enhancement of the kinetic of the CO_2 consumption rate. An increase in the reaction temperatures also favors the reaction pathways implying lower number of protons.

Acknowledgments

Financial Support from the Spanish "Ministerio de Ciencia e Innovación" (Project CTQ2016-75491-R) and from Abengoa Research is gratefully acknowledged. JCSR would like to thank the Spanish Ministry of Economy, Industry, and Competitiveness for financial support through the Ramón y Cajal Program, Grant: RYC-2015-19230.

References

[1] J. Qiao, Y. Liu, F. Hong, J. Zhang, Chem. Soc. Rev. 43 (2014) 631–675.
[2] N.S. Spinner, J.A. Vega, W.E. Mustain, Catal. Sci. Technol. 2 (2012) 19–28.
[3] G.A. Olah, A. Goeppert, G.K.S. Prakash, J. Org. Chem. 74 (2009) 487–498.
[4] M. Mikkelsen, M. Jorgensen, F.C. Krebs, Energ. Environ. Sci. 3 (2010) 43–81.
[5] W. Leitner , Coordin. Chem. Rev. 153 (1996) 257–284.
[6] M. Cheng, E.B. Lobkovsky, G.W. Coates, J. Am. Chem. Soc. 120 (1998) 11018–11019.
[7] I. Omae, Coordin Chem Rev, 256 (2012) 1384–1405.
[8] C. Genovese, C. Ampelli, S. Perathoner, G. Centi, J. Energy Chem. 22 (2013) 202–213.
[9] K. Mori, H. Yamashita, M. Anpo, RSC Adv. 2 (2012) 3165–3172.
[10] C. Oloman, H. Li, ChemSusChem 1 (2008) 385–391.
[11] E.E. Benson, C.P. Kubiak, A.J. Sathrum, J.M. Smieja, Chem. Soc. Rev. 38 (2009) 89–99.
[12] C. Stewart, M.-A. Hessami, Energ. Convers. Manage 46 (2005) 403–420.
[13] V.R. Choudhary, A.M. Rajput, B. Prabhakar, Catal. Lett. 32 (1995) 391–396.
[14] M.C.J. Bradford, M.A. Vannice, Appl. Catal. A: General 142 (1996) 73–96.
[15] J. Ma, N. Sun, X. Zhang, N. Zhao, F. Xiao, W. Wei, Y. Sun, Catal. Today 148 (2009) 221–231.
[16] S.D. Ebbesen, C. Graves, M. Mogensen, Int. J. Green Energy 6 (2009) 646–660.
[17] Y. Hori, Electrochemical CO2 Reduction on Metal Electrodes, in: C. Vayenas, R. White, M. Gamboa-Aldeco (Eds.) Modern Aspects of Electrochemistry, Springer New York 2008, pp. 89–189.
[18] C. Genovese, C. Ampelli, S. Perathoner, G. Centi, J. Catal. 308 (2013) 237–249.
[19] C. Genovese, C. Ampelli, S. Perathoner, G. Centi, Chem. Engineer. Trans. 2013, pp. 289–294.
[20] G. Centi, S. Perathoner, G. Wine, M. Gangeri, Green Chem. 9 (2007) 671–678.
[21] M. Gangeri, S. Perathoner, S. Caudo, G. Centi, J. Amadou, D. Bégin, C. Pham-Huu, M.J. Ledoux, J.P. Tessonnier, D.S. Su, R. Schlögl, Catal. Today 143 (2009) 57–63.
[22] W. Zhang, Y. Hu, L. Ma, G. Zhu, Y. Wang, X. Xue, R. Chen, S. Yang, Z. Jin, Adv. Sci. 5 (2018) 1700275.
[23] C. Jiménez, J. García, R. Camarillo, F. Martínez, J. Rincón, Energ. Fuel. 31 (2017) 3038–3046.
[24] I. Merino-Garcia, J. Albo, A. Irabien, Nanotechnol. 29 (2018) 014001.
[25] E.E. Ortelli, J. Wambach, A. Wokaun, App Catal A: General 216 (2001) 227–241.
[26] T. Inui, H. Matsuda, O. Yamase, H. Nagata, K. Fukuda, T. Ukawa, A. Miyamoto, J. Catal. 98 (1986) 491–501.
[27] D.R. Palo, R.A. Dagle, J.D. Holladay, Chem. Rev. 107 (2007) 3992–4021.
[28] S.G. Jadhav, P.D. Vaidya, B.M. Bhanage, J.B. Joshi, Chem. Eng. Res. Des. 92 (2014) 2557–2567.
[29] J. Toyir, P.R.r. de la Piscina, J.L.G. Fierro, N.s. Homs, Appl. Catal. B: Environmental 29 (2001) 207–215.
[30] J. Liu, J. Shi, D. He, Q. Zhang, X. Wu, Y. Liang, Q. Zhu, Appl. Catal. A: General, 218 (2001) 113–119.
[31] J. Słoczyński, R. Grabowski, P. Olszewski, A. Kozłowska, J. Stoch, M. Lachowska, J. Skrzypek, Appl. Catal. A: General 310 (2006) 127–137.
[32] González, J. A.; Andrés, J. P.; López Antón, R.; De Toro, J. A.; Normile, P. S.; Muñiz, P.; Riveiro, J. M.; Nogués, J. Chem. Mater. 29 (2017) 5200–5206.
[33] J.C. Tokash, B.E. Logan, Int. J. Hydrogen Energ. 36 (2011) 9439–9445.
[34] N. Gutiérrez-Guerra, J.L. Valverde, A. Romero, J.C. Serrano-Ruiz, A. de Lucas-Consuegra, Electrochem. Commun. 81 (2017) 128–131.
[35] Y. Pauleau, F. Thièry, V.V. Uglov, A.K. Kuleshov, S.N. Dub, M.P. Samtsov, Rev. Adv. Mater. Sci. 4 (2003) 139–146.
[36] T. Fuller, E.S.E.T. Division, E.S. Physical, A.E. Division, Elec Soc 2008.
[37] Y. Pauleau, F. Thièry, Mater. Lett. 56 (2002) 1053–1058.
[38] V. Haas, R. Birringer, NanostructMater. 1 (1992) 491–504.
[39] B. Lee, K. Park, H.M. Kim, Int. J. Electrochem. Sci. 8 (2013) 235–248.
[40] A.C. Lee, R.E. Mitchell, T.M. Gür, Solid State Ionics 192 (2011) 607–610.
[41] A. de Lucas-Consuegra, N. Gutiérrez-Guerra, A. Caravaca, J.C. Serrano-Ruiz, J.L. Valverde, Appl Catal A: General 483 (2014) 25–30.

[42] J. Martinez-Frias, A.-Q. Pham, S. M. Aceves, Int. J. Hydrogen Energ. 28 (2003) 483–490.
[43] W. Wang, J. Vohs, R. Gorte, Top Catal. 46 (2007) 380–385.
[44] A. Karelovic, P. Ruiz, Catal. Sci. Technol. 5 (2015) 869–881.
[45] F. Arena, K. Barbera, G. Italiano, G. Bonura, L. Spadaro, F. Frusteri, J. Catal. 249 (2007) 185–194.
[46] Y.-H. Su, Y.-L. Liu, D.-M. Wang, J.-Y. Lai, M.D. Guiver, B. Liu, J. Power Sources 194 (2009) 206–213.
[47] A. Caravaca, A. de Lucas-Consuegra, J. González-Cobos, J.L. Valverde, F. Dorado, Appl. Catal. B: Environ. 113–114 (2012) 192–200.

Graphical abstract

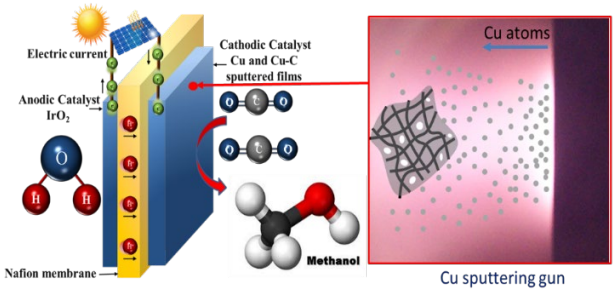

The sputtering technique has been used for the synthesis of Cu based electrodes of low metal loading and high specific activity and selectivity for the electro-reduction of CO_2 to Methanol